Heat Transfer in a Nanofluid Flow Past a Permeable Continuous Moving Non-Isothermal Surface

Falana, A

Mensah, D. J

Department of Mechanical Engineering
University of Ibadan
Ibadan, Nigeria.

Abstract

This study investigates boundary layer for fluid flow and heat transfer characteristics of an incompressible nanofluid flowing over a permeable non-isothermal surface moving continuously. The local similarity solution is applied to the governing equations. The resulting system of non-linear ordinary differential equations is solved numerically using the Runge-Kutta method with shooting techniques. Numerical results for temperature and concentration distributions, as well as the local Nusselt number Nu and local Sherwood number Sh, have been presented for different values of the governing parameters, such as Prandtl number Pr, temperature exponent, n and the velocity ratio, γ .In particular, it has been found that the heat transfer rate is consistently higher for the lower values of the brownian motion parameter (Nb) but decreases for increase in the thermophoresis parameter (Nt). It is further noticed that the mass transfer rate increases for increase in Nb but decreases for increase in Nt.

Keywords: Nanofluid; Non-Isothermal; Thermophoresis; Brownian motion

1. Introduction

The problem of boundary layer flow and heat transfer over a moving or stretching surface is of great importance in view of its relevance in a wide variety of technical applications, particularly in manufacture of fibres in glass production and polymer industries, hot rolling, wire drawing, metal extrusion, continuous casting and paper production, to name a few. The investigation of drag and heat transfer in such cases belong to a separate class of problems in boundary layer theory, distinguishing itself from the study of flows over static surfaces (Ali E.Mohamed [1]; Pop *et al*.,[2]. The resulting flow on a stretched surface emanating from a slit may be modeled as a boundary layer developing away from a slit. Sakiadis [14] was the first to develop a numerical solution for the flow field of a stretched surface using a similarity transformation. As an extension, an exact solution was given by Crane [4] for a boundary layer flow caused by a stretching surface. Since then, many researchers have investigated similar problems with various physical aspects. Olanrewaju, P.O.*et al.* [13] investigated the influence of thermal radiation on the boundary layer flow of nanaofluids over a moving surface in a flowing fluid. The plate is assumed to move in the same or opposite directions to the free stream. They observed that radiation has dominant effect on the heat transfer and the mass transfer rate. Kuznetsov and Nield [8, 9] studied the convective heat transfer in a nanofluid past a vertical plate. They have used a model in which brownian motion and thermophoresis are accounted with simple boundary conditions as in those in which both the temperature and nano particle fraction are constant along the wall.

Bachok, *et al*. [3] studied the steady boundary layer flow of a nanofluid past a moving semi infinite flat plate in a uniform free stream. Xuan and Li [19] experimentally investigated flow and convective heat transfer characteristics for Cu-water based nanofluid through a straight tube with a constant heat flux at the wall. Results showed that the nanofluid gives substantial enhancement of heat transfer rate compared with pure water. Koo and Kleinstreuer [11] studied steady laminar liquid nanofluid flow in micro channels for conduction-convection heat transfer for two different base fluids water and ethylene glycol having copper oxide nano spheres at low volume concentrations.

Hassanien, I.A [7] obtained the boundary layer solutions to the steady flow and heat transfer characteristics of a continuous flat surface moving in a parallel free stream of power-law fluid. Hassanien, I. A *et al.*, [6] have studied the boundary layer analysis for the problem of flow and heat transfer from a power-law fluid to a continuous stretching sheet with variable wall temperature. Meisam M. Habibi and Pouyan Jahangiri [14] studied the forced convection boundary layer MHD flow of nanofluid over a permeable stretching plate with viscous dissipation, the effects of suction and injection and viscous dissipation were taken into account. The model includes Brownian motion and thermophoresis effects, the governing momentum, energy and nanofluid solid volume fraction equations were solved numerically using an explicit finite difference scheme (Keller-box method) and the results were compared with available numerical data. Khan W.A and Pop I. [10] studied the problem of laminar fluid flow which results from the stretching of a flat surface in a nanofluid and investigated it numerically.

Sarvang S.Shan. [16] presented a similarity analysis of the problem of steady boundary layer flow of a nanofluid on a continuous moving permeable isothermal surface. However, it is possible to account for the variations in the temperature of the wall. This extension is the purpose of the present paper.

2. Governing Equations

We consider a flat surface moving with a constant velocity U_w in a parallel direction to a free stream of a nanofluid of uniform velocity U_∞. Either the surface velocity or the free stream velocity may be zero, but not both simultaneously. All physical properties of the fluid are assumed to be constant. It is assumed that at the moving surface, the temperature T and the nanoparticles fraction C take constant values T_w and C_w, respectively while the values of T and C in the ambient fluid are denoted by T_∞ and C_∞, respectively. Following the nanofluid model proposed by Sarvang D. Shah [16], the governing equations of the steady laminar boundary layer flow on the moving surface are given by

$$\frac{\partial u}{\partial x}+\frac{\partial v}{\partial y}=0 \tag{1}$$

$$\frac{u\partial u}{\partial x}+\frac{v\partial u}{\partial y}=-\frac{1}{\rho}\left(\frac{\partial p}{\partial x}\right)+\upsilon\left(\frac{\partial^2 u}{\partial y^2}+\frac{\partial^2 u}{\partial x^2}\right) \tag{2}$$

$$\frac{u\partial T}{\partial x}+\frac{v\partial T}{\partial y}=\alpha\left(\frac{\partial^2 T}{\partial y^2}+\frac{\partial^2 T}{\partial x^2}\right)+\tau\left[D_b\left(\frac{\partial C}{\partial x}\frac{\partial T}{\partial x}+\frac{\partial C}{\partial y}\frac{\partial T}{\partial y}\right)+\left(D_T/T_\infty\right)\left\{\left(\frac{\partial T}{\partial x}\right)^2+\left(\frac{\partial T}{\partial y}\right)^2\right\}\right] \tag{3}$$

$$\frac{u\partial u}{\partial x}+\frac{v\partial u}{\partial y}=D_b\left(\frac{\partial^2 C}{\partial x^2}+\frac{\partial^2 C}{\partial y^2}\right)+\left(\frac{D_T}{T_\infty}\right)\left(\frac{\partial^2 T}{\partial x^2}+\frac{\partial^2 T}{\partial y^2}\right) \tag{4}$$

where u and v are the velocity components along the x and y axes, respectively, $\alpha = \kappa/(\rho c)$ is the thermal diffusivity of the fluid, ν is the kinematic viscosity coefficient and κ is the thermal conductivity and $\tau=(\rho C)p/(\rho C)f$

The Boundary conditions are given by,

$$y=0: u=u_w\ ;\ v=v_w, T=T_w\ ;\ C=C_w$$

$$y\longrightarrow\infty: u=u_\infty;\ T=T_\infty,\ C=C_\infty \tag{5}$$

The boundary conditions $u = u_w$ represents the case of a plane surface moving in parallel to the free stream. Here we introduce the stream function, $\psi(x,y)$ such that:

$$u=\frac{\partial\psi}{\partial y} \quad \text{and} \quad v=\frac{\partial\psi}{\partial x} \tag{6}$$

which identically satisfies equation (1).

To analyze the effect of both the moving wall with stagnant free stream and stationary wall with a uniform free stream velocity, we introduce a new similarity coordinate and a dimensionless stream function. Following Sarvang S.D. [16],

$$\eta = \frac{y}{x}\left(\mathrm{Re}_w + \mathrm{Re}_\infty\right)^{1/2}; \qquad f = \frac{\psi(x,y)}{\nu\left(\mathrm{Re}_w + \mathrm{Re}_\infty\right)^{1/2}} \tag{7}$$

which are the combinations of the traditional ones:

$$\eta_B = \frac{y}{x}\left(\mathrm{Re}_\infty^{\frac{1}{2}}\right); \qquad f_B = \frac{\psi(x,y)}{\left(\nu\,\mathrm{Re}_\infty^{\frac{1}{2}}\right)}$$

$$\eta_s = \frac{y}{x}\left(\mathrm{Re}_w^{\frac{1}{2}}\right); \qquad f_s = \frac{\psi(x,y)}{\left(\nu\,\mathrm{Re}_w^{\frac{1}{2}}\right)} \tag{8}$$

$$\mathrm{Re}_w = \frac{u_w x}{\nu}; \qquad \textit{and} \qquad \mathrm{Re}_\infty = \frac{u_\infty x}{\nu}$$

A velocity ratio parameter γ is defined as

$$\gamma = \frac{u_w}{\left(u_w + u_\infty\right)} = \left(1 + \frac{u_w}{u_\infty}\right)^{-1} = \left(1 + \frac{R_\infty}{\mathrm{Re}_w}\right)^{-1}$$

Note that for Blasius problem, $u_w = 0$ therefore $\gamma = 0$ while for the Sakiadis case, $u_\infty = 0$ and thus $\gamma = 1$.

Furthermore, the dimensionless temperature and concentration functions are defined as:

$$\theta(\eta) = \left(T - T_\infty\right)/\left(T_w - T_\infty\right)$$

$$\phi(\eta) = \left(C - C_\infty\right)/\left(C_w - C_\infty\right) \tag{9}$$

Using the transformation variables defined in equations, (6)-(9), Equations (2)-(4) reduce to

$$f''' + \frac{1}{2} f f'' = 0 \tag{10}$$

$$\frac{\theta''}{P_r} + \frac{f\theta'}{2} + N_b \phi'\theta' + N_t\left(\theta'\right)^2 - n\theta f' = 0 \tag{11}$$

$$\phi'' + \frac{L_e f\phi'}{2} + \frac{N_t}{N_b}\theta'' = 0 \tag{12}$$

where prime denotes differentiation with respect to η.

The transformed boundary conditions are given by

$$f(0) = f_w, \quad f'(0) = \gamma, \quad \theta(0) = 1, \quad \phi(0) = 1$$

$$f'(\infty)\ 1-\gamma, \quad \theta(\infty) = 0, \quad \phi(\infty) = 0 \tag{13}$$

Four parameters are defined by

$P_r = \frac{\nu}{\alpha}$ (Prandtl number); $Le = \frac{\nu}{D_b}$ (Lewis number);

$N_b = \left[\frac{\left(\rho C\right)_p D_b\left(\phi_w - \phi_\infty\right)}{\left(\rho C\right)_f \upsilon}\right]$ (Brownian motion parameter) and

$$N_t = \left[\frac{\left(\rho C\right)_p D_T\left(T_w - T_\infty\right)}{\left(\rho C\right)_f T_\infty \nu}\right] \text{(Thermophoresis parameter).} \tag{14}$$

We notice that when n =0 (i. e., temperature exponent for the non-isothermal case is zero) equation (11) reduces to the equation considered by Sarvang D.Shah [16]. Similarly, when Nb =Nt =0, this boundary value problem reduces to the classical problem of heat and mass transfer due to a stretching surface in a viscous fluid.

3 Heat and mass transfer coefficients

The local heat flux at the wall is given by:

$$q_w = -\kappa\left[\frac{\partial T}{\partial y}\right]_{y=0} \quad (15)$$

The local Nusselt number is defined as:

$$Nu_x = \frac{q_w x}{\kappa(T_w - T_\infty)} \quad (16)$$

where κ is the effective thermal conductivity of the nanofluid.

Using equation (15) in equation (16), the dimensionless Nusselt number can be represented as

$$Nu_x = -(\mathrm{Re}_w - \mathrm{Re}_\infty)^{\frac{1}{2}}\theta'(0) \quad (17)$$

The mass flux at the wall is given by:

$$q_m = -D_b\left[\frac{\partial C}{\partial y}\right]_{y=0} \quad (18)$$

The Local Sherwood number is defined as:

$$Sh_x = \frac{q_m x}{D_b(C_w - C_\infty)} \quad (19))$$

Using (18) in (19) the dimensionless Sherwood number is obtained as

$$Sh_x = -(\mathrm{Re}_w - \mathrm{Re}_\infty)^{\frac{1}{2}}\phi'(o) \quad (20)$$

4. Solution Methodology

The set of nonlinear ordinary differential equation (10)-(12) which satisfies the boundary conditions (13) were integrated numerically using the fourth order Runge-kutta scheme along with a systematic guessing of $f''(0),\ \theta'(0)\ and\ \phi'(0)$ by the shooting technique until the boundary conditions at infinity $f''(\infty),\ \theta'(\infty)\ and\ \phi'(\infty)$ decay exponentially to zero. The computations have been done using Matlab, and accuracy to the fourth decimal place is sufficient for convergence. The effect of heat and mass transfer in nanofluid flow past a non-isothermal permeable surface has been studied for different values of Brownian motion parameter (Nb) and thermophoresis parameter (Nt) along with other parameters like the Prandtl number (Pr) and Lewis number (Le).

5. Results and Discussion

To check the accuracy of the present work, solutions are obtained for the reduced Nusselt number $-\theta'(0)$ by ignoring the effect of Nt and Nb. The result is compared with the results reported by Sarvang S. Shah [16], Gorla and Sidawi [5], and Wang [18] when Nt=Nb=0 and γ=1 in Table 1. The results are in good agreement and this confirms the accuracy of our numerical procedure.

Table 1: Comparison of Wall Temperature Gradient, $-\theta'(0)$ for Different Values of Pr for Sakiadis Problem (Nt = Nb =0, $\gamma = 1$)

Prandtl number	Present Result	Wang(1989)	Gorla and Sidawi(1994)	Sarvang, S. Shah(2010)
0.07	0.06570	0.0656	0.0656	0.0656
0.2	0.16930	0.1691	0.1691	0.1691
0.7	0.45410	0.4539	0.4539	0.4539
7	1.89580	1.8954	1.8905	1.8907
20	3.35500	3.3539	3.3539	3.3539

Table 2: Variation of Nu and Sh with Nt and Nb for Various Values of n, Le when γ =0 and Pr=0.7

n	γ	Le	Nt	$-\theta'(0)$				$-\phi'(0)$		
				Nb=0.1	Nb=0.2	Nb=0.3		Nb=0.1	Nb=0.2	Nb=0.3
			0.1	0.30107	0.29063	0.28158		0.23250	0.2841	0.2883
0.1	0	1	0.2	0.29368	0.28350	0.27364		0.14930	0.2470	0.2773
			0.3	0.28628	0.27521	0.26650		0.07615	0.2163	0.2615
		5	0.1	0.29607	0.28215	0.26875		0.53025	0.5568	0.5663
			0.2	0.28721	0.27370	0.26077		0.49858	0.5458	0.5601
			0.3	0.27906	0.26607	0.25318		0.45997	0.5281	0.5565
0.3		1	0.1	0.34767	0.33738	0.32653		0.19950	0.2634	0.2935
			0.2	0.33990	0.32941	0.31915		0.07890	0.2144	0.2595
			0.3	0.33076	0.32203	0.31195		0.00106	0.1650	0.2285
		5	0.1	0.34153	0.32668	0.31231		0.49961	0.5450	0.5595
			0.2	0.33207	0.31773	0.30382		0.44985	0.5223	0.5475
			0.3	0.32307	0.30926	0.29570		0.40535	0.5018	0.5373
0.5		1	0.1	0.38561	0.37484	0.36431		0.16999	0.2550	0.2833
			0.2	0.37758	0.36702	0.35670		0.02306	0.1860	0.2400
			0.3	0.36653	0.35938	0.34903		0.00094	0.1234	0.2036
		5	0.1	0.37852	0.36359	0.34840		0.48675	0.5384	0.5520
			0.2	0.36870	0.35432	0.33948		0.41200	0.4900	0.5328
			0.3	0.35942	0.34476	0.34470		0.34150	0.4765	0.4775

Table 3: Variation of Nu and Sh with Nt and Nb for various values of n, Le at γ =0 and Pr=0.7

n	γ	Le	Nt	$-\theta'(0)$				$-\phi'(0)$		
				Nb=0.1	Nb=0.2	Nb=0.3		Nb=0.1	Nb=0.2	Nb=0.3
			0.1	0.24060	0.23035	0.22033		0.27815	0.30880	0.31902
-0.1	0	1	0.2	0.23325	0.22304	0.21266		0.23610	0.29158	0.30980
			0.3	0.22608	0.21610	0.20636		0.20455	0.27963	0.30425
		5	0.1	0.23695	0.22433	0.21208		0.56028	0.57200	0.57623
			0.2	0.22869	0.21625	0.20470		0.55473	0.57350	0.57970
			0.3	0.21978	0.20858	0.19150		0.55760	0.57875	0.59850
-0.3		1	0.1	0.15110	0.14120	0.13178		0.33995	0.33935	0.33895
			0.2	0.14350	0.13400	0.12470		0.35883	0.35199	0.34973
			0.3	0.13600	0.12690	0.11780		0.38740	0.36948	0.36328
		5	0.1	0.14970	0.13950	0.12990		0.59988	0.59103	0.58780
			0.2	0.14160	0.13175	0.12250		0.63165	0.60981	0.60175
			0.3	0.13355	0.12430	0.11545		0.66993	0.63140	0.61825
-0.5		1	0.1	0.03655	0.02705	0.01850		0.41513	0.37625	0.36295
			0.2	0.02750	0.01925	0.01050		0.50975	0.42580	0.39805
			0.3	0.01675	0.00986	0.00203		0.61743	0.48128	0.43605
		5	0.1	0.03900	0.03285	0.02725		0.64513	0.61203	0.60055
			0.2	0.02835	0.02255	0.01735		0.72205	0.65150	0.62795
			0.3	0.01730	0.01215	0.00750		0.80625	0.69450	0.65688

Tables 2 and 3 above display the values at the wall for heat transfer rate, $-\theta'(0)$ and the mass transfer rate, $-\phi'(0)$. They are proportional to our Nusselt number and Sherwood number respectively. Tables 2 and 3 represent the boundary layer flow over a stationary surface with a uniform free stream velocity (Blasius case) where we have our velocity ratio as zero $(\gamma = 0)$. Other parameters like the Lewis number and Prandtl number are varied to observe the trend on the resulting heat and mass transfer rates. The results indicate that when the wall's surface temperature exponent is positive (n > 0), increasing Nb results in decrease in the heat transfer rate and increase mass transfer rate.

With an increase in Nt, there is a decrease in heat and mass transfer rates from the surface. Moreover, when the wall temperature exponent, n becomes increasingly negative (n < 0), increase in Nb and Nt results in decrease in the heat transfer rates whereas the mass transfer rate increases with Nt. Calculations show that these conclusions are also true for the Sakiadis case $(\gamma = 1)$.

In order to get a physical insight into the problem, the effects of various physical and fluid parameters are shown graphically in figures 1-21.

Figures 1, 2 illustrate (for the Sakiadis problem, where $\gamma = 1$) the variation of Nb on the temperature and concentration profiles for both positive and negative values of the temperature exponent, n for constant Nt and Pr. It is observed that as Nb increases the temperature increases and the concentration decreases gradually for positive temperature exponent (n= 0.5).The thermal boundary layer thickness is smaller than concentration boundary layer thickness. However, for negative temperature exponents (n= – 0.1), as Nb increases the temperature increases and the concentration decreases more rapidly. The thickness of the boundary layer for concentration is smaller than the thermal boundary layer thickness.

In figures 3, 4 (for the Blasius problem, where $\gamma = 0$), as Nb increases, the temperature increases while the concentration decreases for positive temperature exponent (n=0.5).The thermal boundary layer thickness is therefore smaller than the concentration boundary layer thickness. But for negative temperature exponent (n= -0.3), as Nb increases the temperature increases and the concentration decreases very rapidly. Here, the concentration boundary layer thickness is smaller than the thermal boundary layer thickness.

In figures 5, 6 where $(\gamma = 1)$, the variation of Nt for constant values of Nb, Pr, positive and negative values of n are shown. As Nt increase for positive n, (n= 0.1), the temperature increases and the concentration increases. For negative n, (n= -0.5), as Nt increases the temperature increases and the concentration increases.

In figures 7 – 9 where $(\gamma = 0)$, as Nt increases both temperature and concentration increases for positive n, (n= 0.1) and for higher n, (n= 0.5) concentration increases more rapidly. But for negative n, (n= – 0.5), temperature increases more rapidly while concentration decreases.

Figures 10-11 where $(\gamma = 1)$, illustrate the concentration profile for various Lewis numbers (Le). It is observed that as Le increases, the concentration decreases and the concentration boundary layer thickness decreases. This means that the surface mass transfer rate increases as Le increases. The same observation is true for the case $\gamma = 0$.

Figures 12, 13 show the temperature distribution as the Prandtl number, Pr increases. As Pr increases, we observed that the temperature decreases and the thermal boundary layer thickness decreases. This means that the surface heat transfer rate increases as Pr increases. This observation is true for both cases $\gamma = 1$, and $\gamma = 0$ respectively.

Figures 14–21 show the variation of heat and mass transfer rates as Nb and Nt increase for both positive and negative values of n, for the cases $\gamma = 1$ and $\gamma = 0$.

In figures14–15 where $(\gamma = 1)$, the heat transfer rates decreases as Nb or Nt increases and the decrease is more rapid for negative n.

In figures 16–17 where $(\gamma = 1)$, the mass transfer rates increases as Nb or Nt increases for positive n, but the mass transfer rates decreases as Nb or Nt increases for negative n.

Figures 18–19 where $(\gamma = 0)$ show that the heat transfer rates decreases as Nb or Nt increases for both positive and negative values of n. Also, the mass transfer rates increases as Nb or Nt increases for positive n (see figure20), but decreases as Nb or Nt increases for negative values of n (see figure 21).

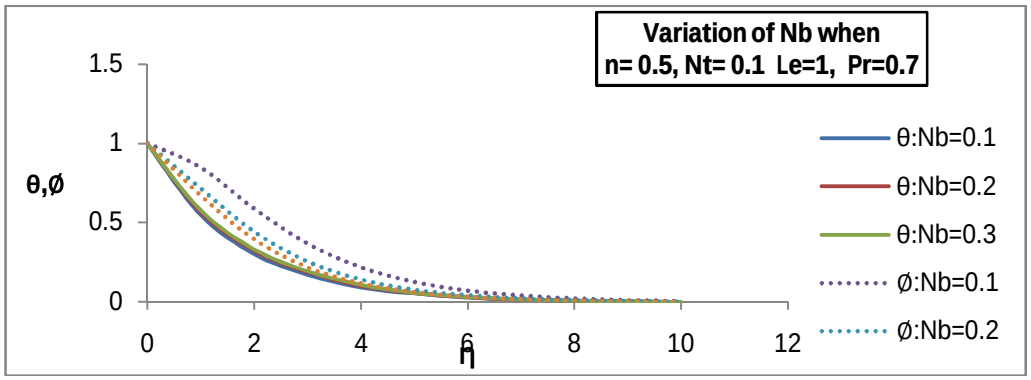

Figure 1: Temperature and Concentration Profiles for Different Values of Nb with $(\gamma = 1)$

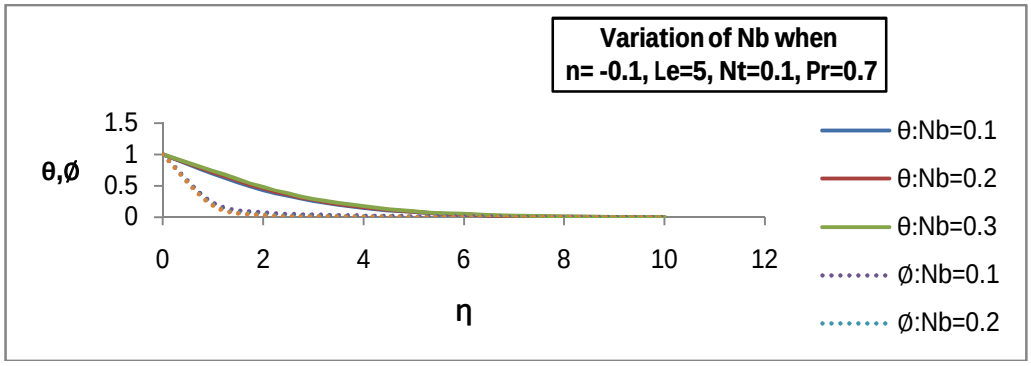

Figure 2: Temperature and Concentration Profiles for Different Values Of Nb with $(\gamma = 1)$

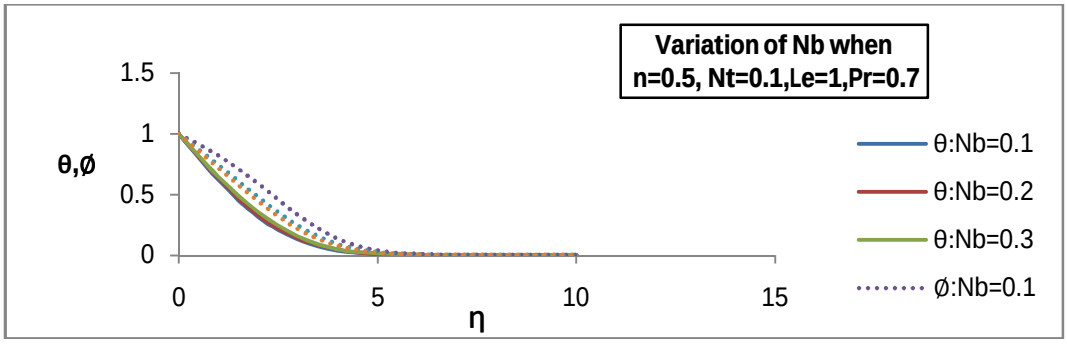

Figure 3: Temperature and Concentration Profiles for Different Values of Nb with $(\gamma = 0)$

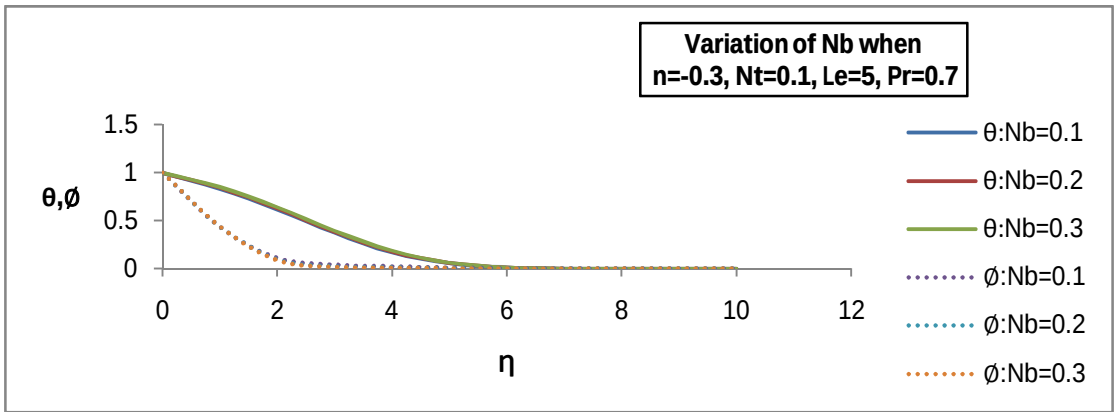

Figure 4: Temperature and Concentration Profiles for Different Values of Nb with $(\gamma = 0)$

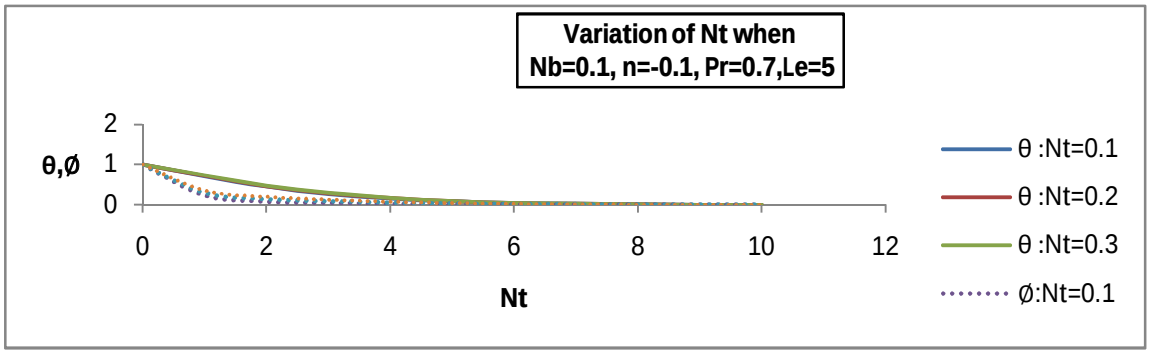

Figure 5: Temperature and Concentration Profiles for Different Values of Nt with $(\gamma = 1)$

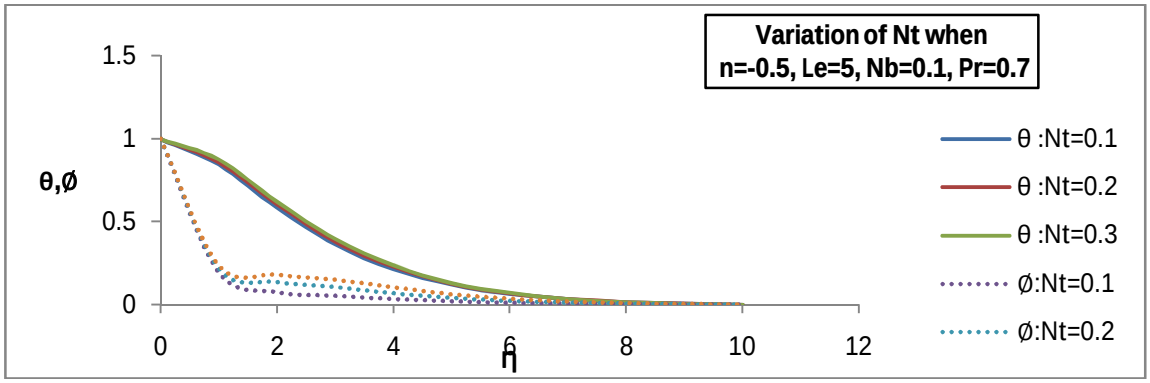

Figure 6: Temperature and Concentration Profiles for Different Values of Nt with $(\gamma = 1)$

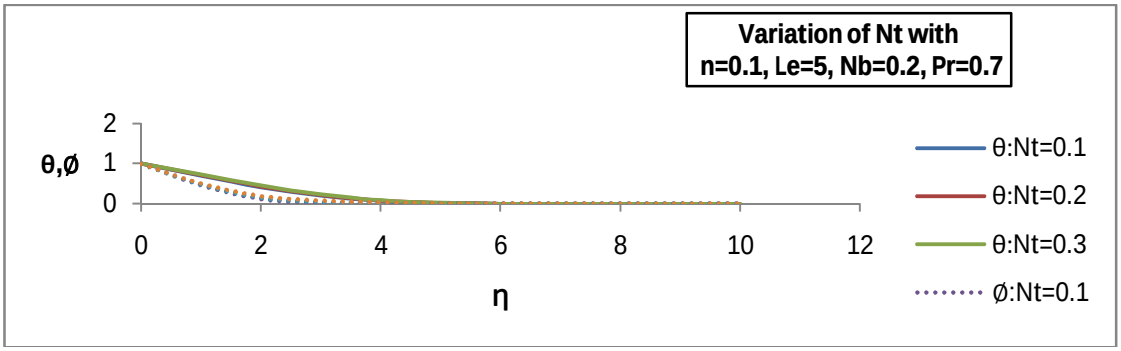

Figure 7: Temperature and Concentration Profiles for Different Values of Nt with $(\gamma = 0)$

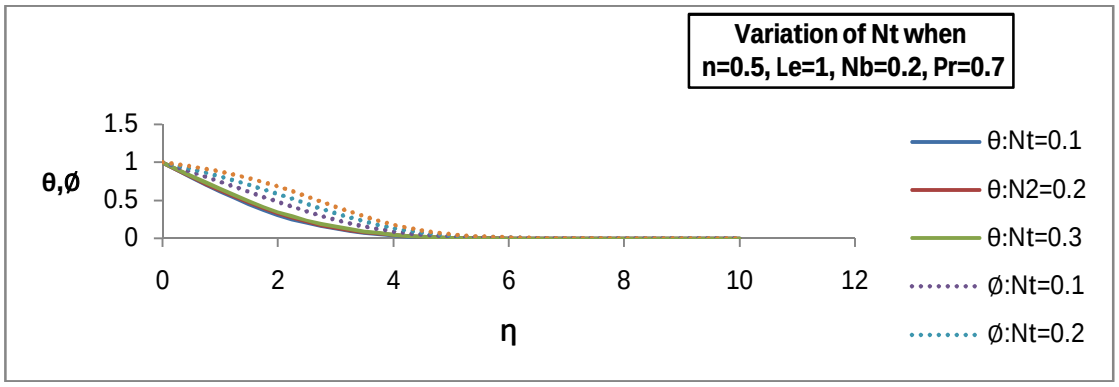

Figure 8: Temperature and Concentration Profiles for Different Values of Nt with $(\gamma = 0)$

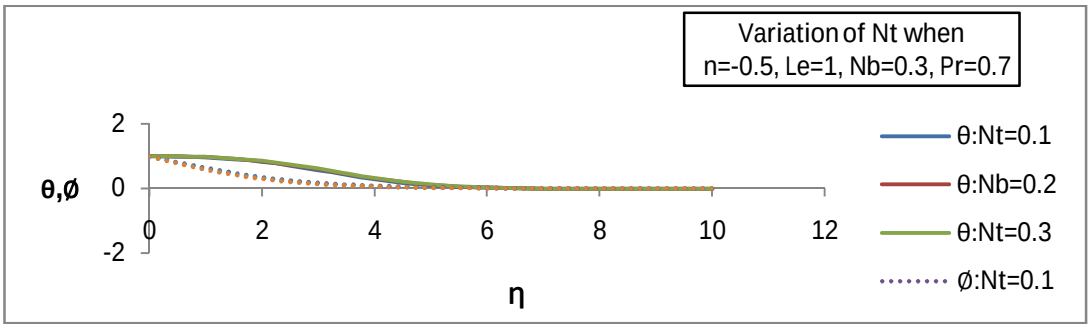

Figure 9: Temperature and Concentration Profiles for Different Values of Nt with $(\gamma = 0)$

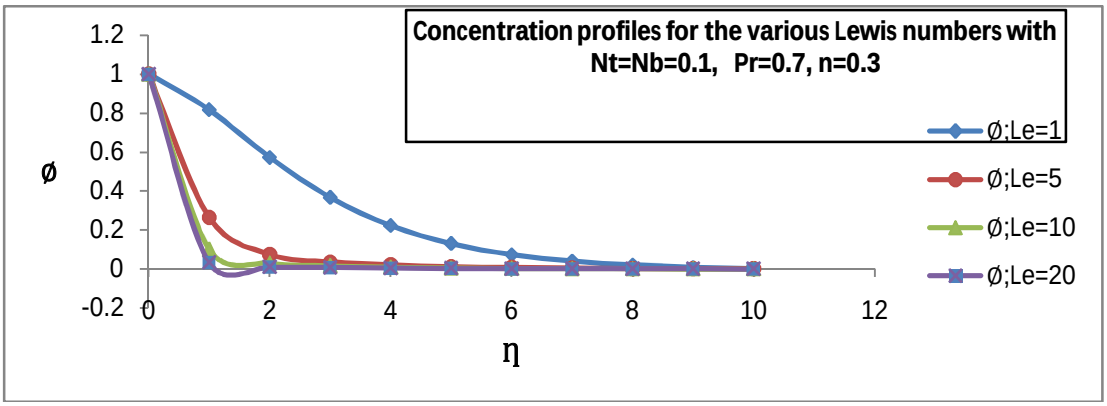

Figure 10: Concentration Profiles for the Various Lewis Numbers with $(\gamma = 1)$

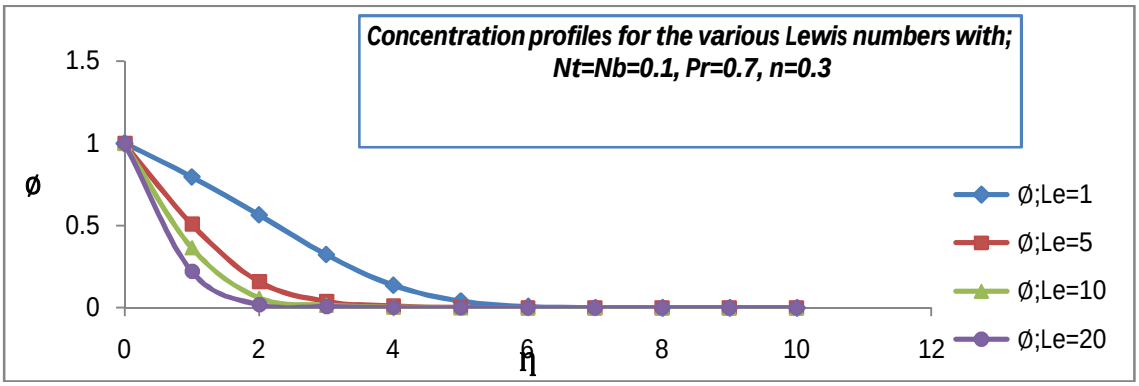

Figure 11 Concentration Profiles for the Various Lewis Numbers with $(\gamma = 0)$

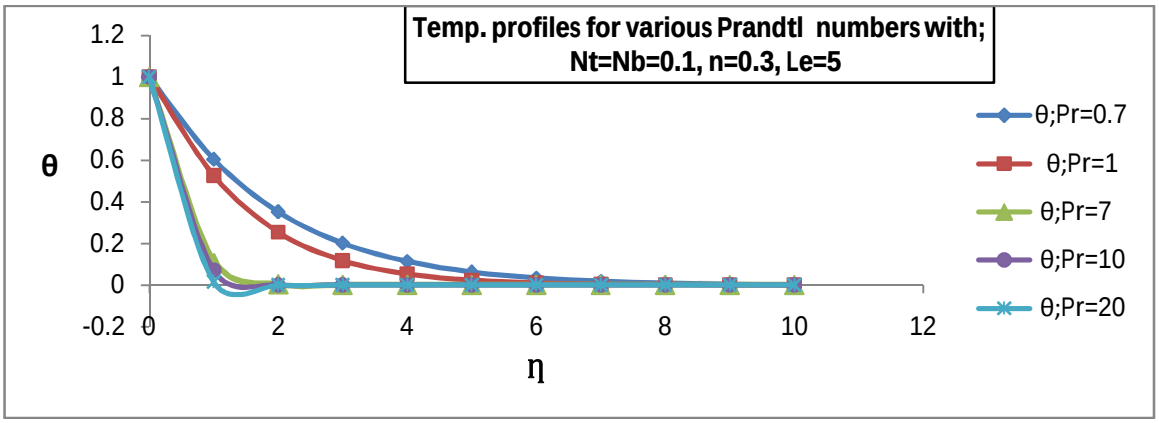

Figure12: Temperature Profiles for Various Prandtl Numbers with $\gamma = 1$

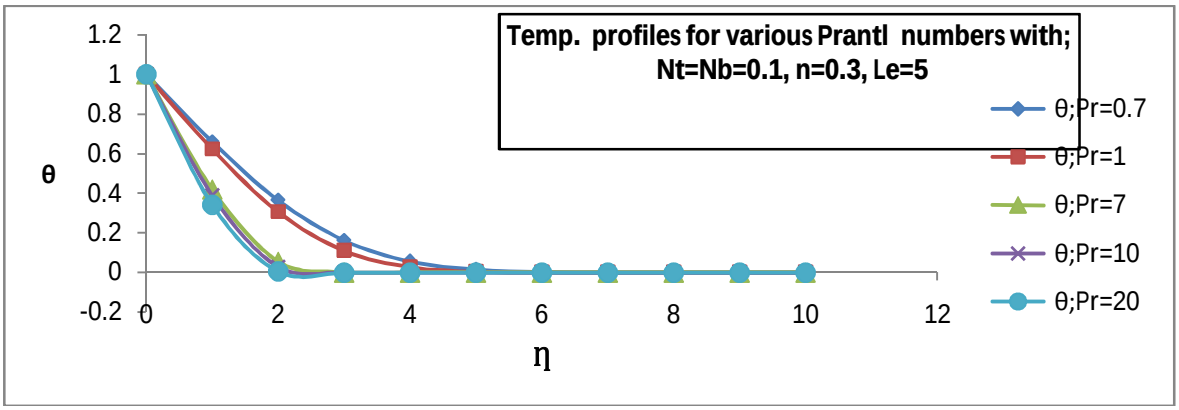

Figure 13: Temperature Profiles for Various Prandtl Numbers with $\gamma = 0$

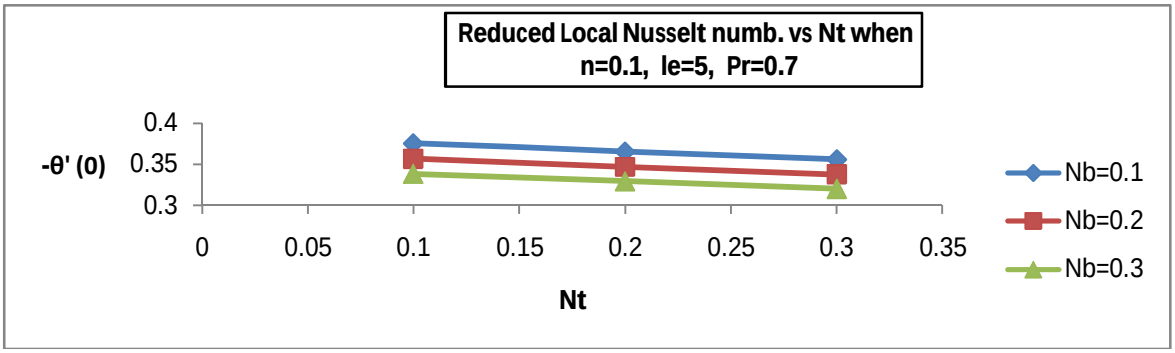

Figure 14: Showing Reduced Local Nusselt Number vs. Nt with $\gamma = 1$

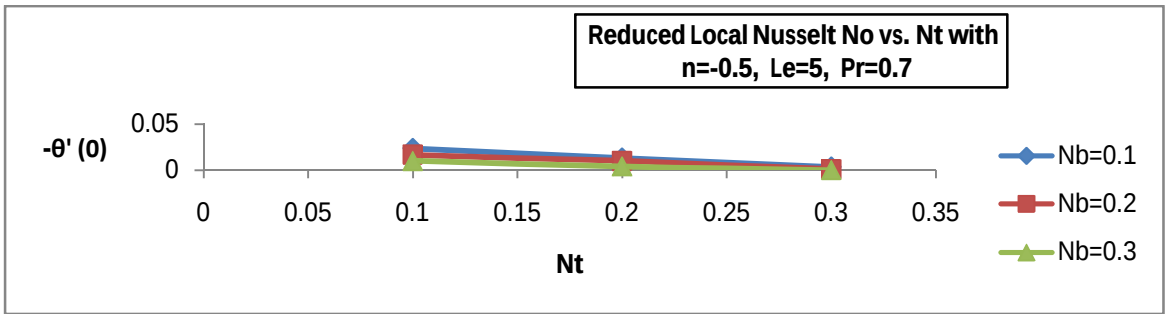

Figure 15: Showing the Reduced local Nusselt Number and Nt with $\gamma = 1$

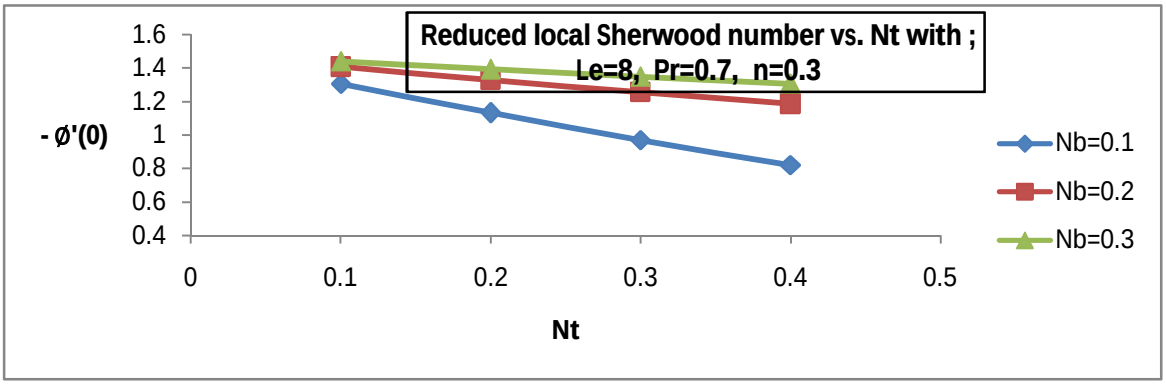

Figure 16: Showing the Reduced Local Sherwood Number vs. Nt with $\gamma = 1$

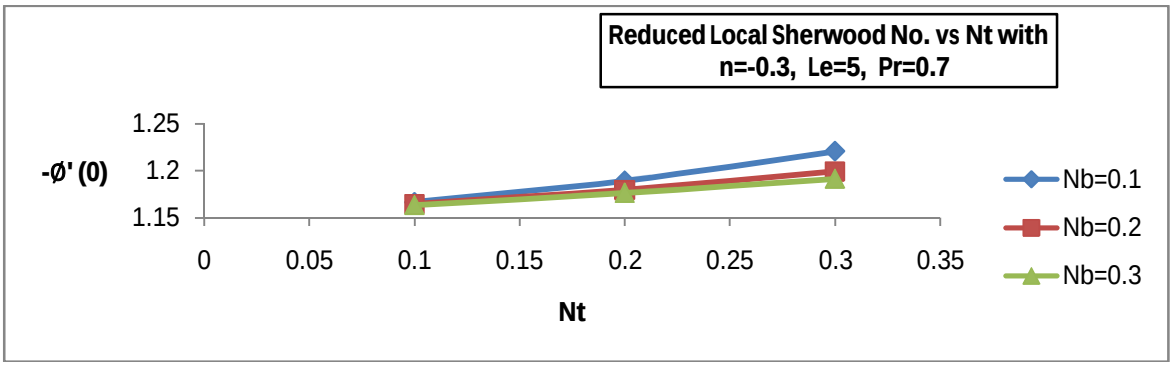

Figure 17: Showing Reduced Local Sherwood Number vs. Nt with $\gamma = 1$

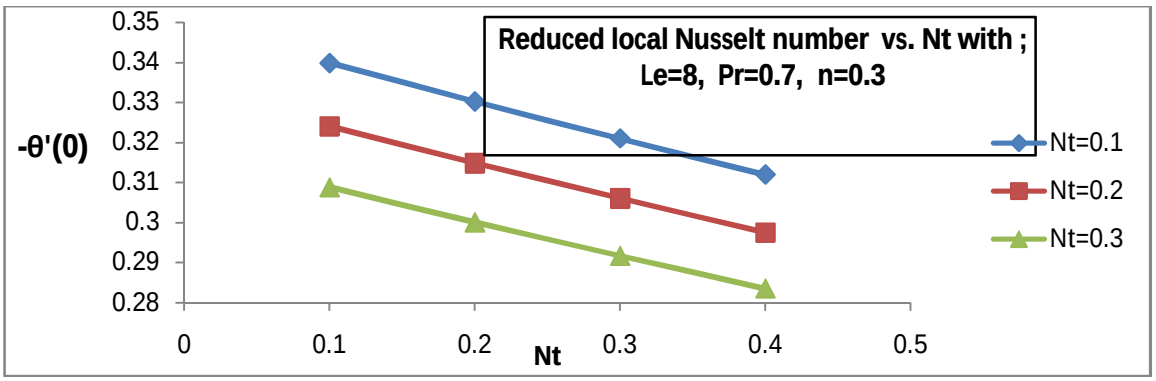

Figure 18: Showing the Reduced Local Nusselt Number vs. Nt with $\gamma = 0$

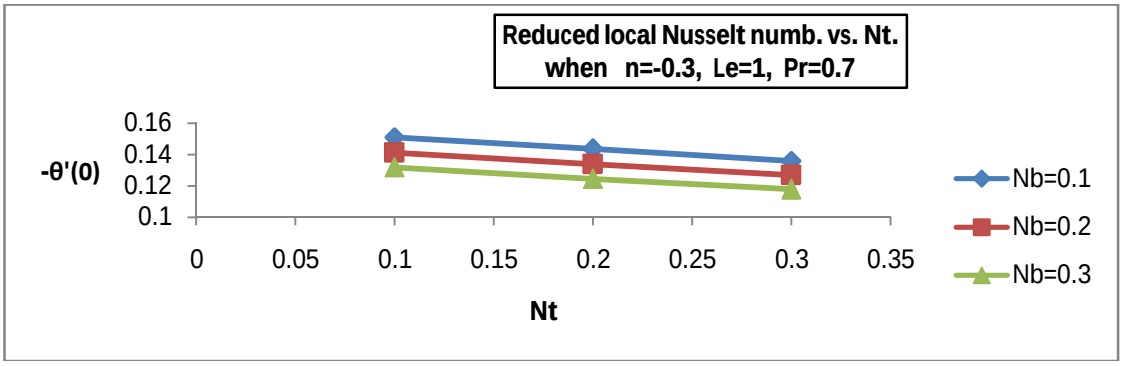

Figure 19: Showing Reduced Local Nusselt Number vs. Nt with $\gamma = 0$

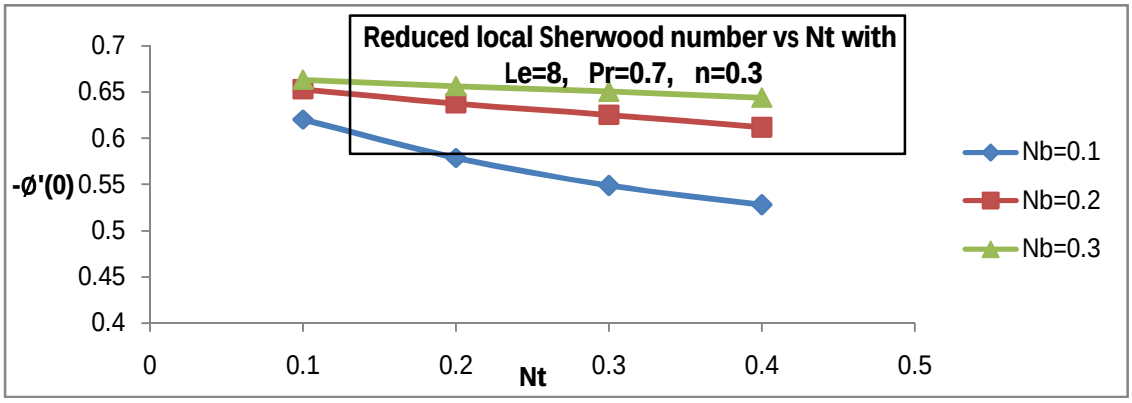

Figure 20: Showing the Reduced local Sherwood Number vs. Nt with $\gamma = 0$

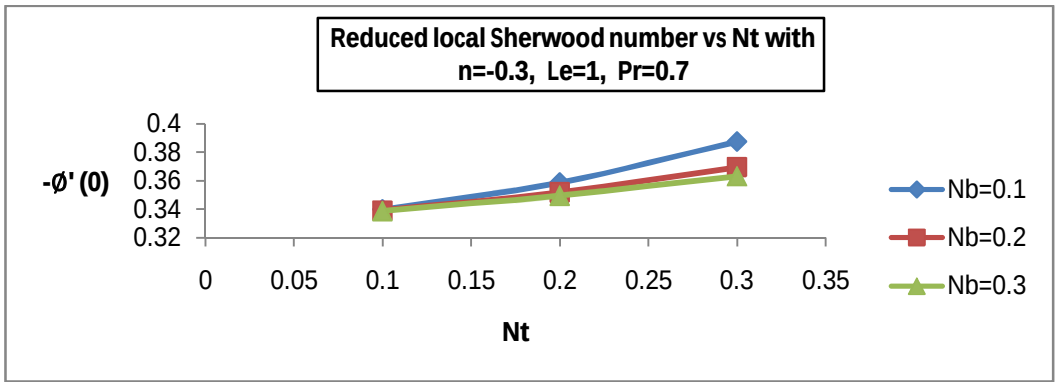

Figure 21: Showing Reduced Local Sherwood Number vs. Nt with $\gamma = 0$

6. Conclusions

It this work, we have studied the problem of heat transfer in a nanofluid past a permeable continuous moving non-isothermal surface. The governing boundary layer equations are solved numerically using the fourth –order Runge-Kutta scheme with shooting technique. The development of the Nusselt number and Sherwood number as well as the temperature and concentration distributions for various values of the velocity ratio, the temperature exponent, and nanaofluid parameters has been discussed and illustrated in tables and graphs. The results indicate that the local Nusselt number is consistently higher for the lower values of the Brownian motion parameter but decreases for increase in the thermophoresis parameter.

References

[1]. Ali E. Mohamed, 1995. On thermal boundary layer on a power-law stretched surface with sunction or injection. Int. J. Heat and Fluid Flow 16:280-290.

[2]. Bachok, N., Ishak, A. and Pop, I., 2010. Boundary-layer Flow of Nanofluids over a Moving Surface in a Flowing Fluid. *Int. J. of Thermal Sciences*, VOl. 49, pp. 1663 – 1668.

[3]. Crane, L. J., 1970. Flow Past a Stretching Plate," *ZAMP*, Vol. 21, pp. 645 – 647.

[4]. Gorla, R.S.R. and Sidawi, I., 1994. Free Convection on a Vertical Stretching Surface with Suction and Blowing*," Applied Scientific Research*, Vol. 52, pp. 247 – 257.

[5]. Hassanien, I.A., Abdullah, A. and Gorla, R. S. R., 1998. Flow and heat transfer in a Power- Law Fluid over a Non-isothermal Stretching Sheet. *Mathl. Comput. Modelling*, Vol. 28, pp. 105 – 116.

[6]. Hassanien, I.A., 1996**.** Flow and Heat Transfer on a Continuous Flat Surface Moving in a Parallel Free Stream of Power-Law Fluid. *Appl. Math. Modelling*, Vol. 20, pp.779 – 784.

[7]. Pop, I. *et al*. Laminar Boundary Layer Flow and Heat Transfer along a Moving Cylinder with Sunction or Injection. TECHNISCHE MECHANIK, Band 15, Heft 2, (1995), pp. 99-106.

[8]. Kuznetsov, A.V., and Nield, D.A., 2010**.** Natural Convective Boundary-layer Flow of a Nanofluid Past a Vertical Plate. *Int. J. of Thermal Sciences*, Vol. 49, pp. 243 – 247.

[9]. Kuznetsov, A.V., and Nield, D.A., 2009**.** The Cheng–Minkowycz Problem for Natural Convective Boundary-layer Flow in a Porous Medium Saturated by a Nanofluid. *Int. J. of Heat and Mass Transfer*, Vol. 52, pp. 5792 – 5795.

[10].Khan,W.A. and Pop, I.,2010. Boundary-Layer Flow of a Nanofluid Past a Stretching Sheet. *International Journal of Heat and Mass Transfer*, Vol. 53,pp. 2477 – 2483.

[11].Koo, J. and Kleinstreuer, C., 2005**.** Laminar Nanofluid Flow in Microheat –Sinks. *International Journal of Heat and Mass Transfer*, Vol. 48, pp. 2652 – 2661.

[12].Olajuwon, B.I., 2009**.** Flow and Natural Convection Heat Transfer in a Power Law Fluid Past a Vertical Plate with Heat Generation. *Int. J. of Nonlinear Science* Vol.7, pp. 50 – 56.

[13].Olanrewaju, P.O. *et al*, 2012. Boundary Layer Flow of Nanofluids Over a Moving Surface in a Flowing Fluid in the Prescence of Radiation. Int.J. of Applied Science and Technology, vol. 2, 2012.

[14].Pouyan, J. and Habibi M. M., 2008 MHD Flow of Nanofluid Over a Permeable StretchingPlate with Viscous Dissipation.

[15].Sakiadis, B. C.,1961.Boundary-layer behaviour on a continuous solid surface: II-The boundary layer on a continuous flat surface. *AIChE Journal*, Vol. 7, pp. 221 – 225.

[16].Sarvang D. Shah, 2010 "Heat Transfer in a Nanofluid Flow Past a Permeable Continuous Moving Isothermal Surface". MSc. Project, Cleveland state University.

[17].Tsou, F. K., Sparrow, E. M. and Goldstein, R. J., 1960.Flow and Heat Transfer in The Boundary Layer in the Continuous Moving Surfaces. *Int. J. Heat Mass Transfer*, Vol. 10, 1967, pp. 219 – 235.

[18].Wang, C.Y., 1989.Free Convection on a Vertical Stretching Surface. *ZAMM*, Vol. 69, pp. 418 – 420.

[19].Xuan,Y. and Li, Q.,2003.Investigation on Convective Heat Transfer and Flow Features of Nanofluids. *Journal of Heat Transfer*, Vol. 125, pp. 151 – 155.

[20].Xuan, Y., Li, Q., and Hu, W., 2010.Aggregation Structure and Thermal Conductivity of Nanofluids," *AIChE Journal*, vol. 49, no. 4, pp. 1038–1043, 2003 , vol. 10, no. 8, pp. 4824-4849.